General Disclaimer

One or more of the Following Statements may affect this Document

- This document has been reproduced from the best copy furnished by the organizational source. It is being released in the interest of making available as much information as possible.

- This document may contain data, which exceeds the sheet parameters. It was furnished in this condition by the organizational source and is the best copy available.

- This document may contain tone-on-tone or color graphs, charts and/or pictures, which have been reproduced in black and white.

- This document is paginated as submitted by the original source.

- Portions of this document are not fully legible due to the historical nature of some of the material. However, it is the best reproduction available from the original submission.

NASA Technical Memorandum 82959

Polyimides—Tribological Properties and Their Use as Lubricants

Robert L. Fusaro
Lewis Research Center
Cleveland, Ohio

Prepared for the
First Technical Conference on Polyimides
sponsored by the Society of Plastics Engineers, Inc.
Ellenville, New York, November 10-12, 1982

NASA

POLYIMIDES - TRIBOLOGICAL PROPERTIES AND THEIR USE AS LUBRICANTS

Robert L. Fusaro

National Aeronautics and Space Administration
Lewis Research Center
Cleveland, Ohio 44135

Friction, wear, and wear mechanisms of several different polyimide films, solid bodies, composites, and bonded solid lubricant films are compared and discussed. In addition, the effect of such parameters as temperatures, type of atmosphere, contact stress, and specimen configuration are investigated. A friction and wear transition occurs in some polyimides at elevated temperatures and this transition is related to molecular relaxations that occur in polyimide. Friction and wear data from an accelerated test (pin-on-disk) are compared to similar data from an end use test device (plain spherical bearing), and to other polymers investigated in a similar geometry.

INTRODUCTION

The use of polymers for tribological applications is continually increasing. In addition, technology is placing ever increasing performance demands on polymers used for tribological applications. Polymers are needed which have improved mechanical properties from cryogenic to the highest possible temperature. One class of thermally stable organic polymers which has demonstrated increased capabilities in these areas is polyimide.

The word polyimide is a generic designation and refers to a class of long-chained polymers which have repeating imide groups as an intergal part of the main chain. By varying the monomeric starting materials, polyimides of different chemical composition and structure can be obtained. The polyimide chains consist of aromatic rings alternated with heterocyclic groups and due to multiple bonds between these groups, the polyimides are characterized by a high thermal stability. At the decomposition point, they crumble to a fine powder without melting. They have a high radiation stability and can stand exposure to neutrons, electrons, ultraviolet light, and gamma radiation. They are resistent to most common chemicals and solvents, but are attacked by alkalis. For a more detailed discussion of the physical properties, see references 1 to 5.

Polyimides are being considered for use in bearings, gears, seals, and prosthetic human joints[6-12]. The intended end use part can be machined or molded from the polyimide or a film of polyimide may be applied to a metallic part. In many instances, polyimide by itself will be sufficient to improve the tribological properties of the intend end use component. However, in some cases, solid lubricant additives may be needed to improve lubrication. To improve the load carrying capacity of polyimide solid bodies, they can be reinforced with fibers. If graphite fibers are used, in addition to improving the strength and stiffness of the polyimide, improved lubricating performances can be obtained, due to the graphite fibers good tribological properties[13-19].

In order to propitiously use polyimides for tribological applications, mechanisms of lubrication and wear, and the factors effecting those mechanisms must be clearly understood. This paper will review the work to date conducted at NASA Lewis Research Center on the fundamental aspects of polyimide lubrication. In addition, tribological materials formulated at Lewis for specific end use applications with polyimide as the matrix material will be discussed.

MATERIALS

Nine different polyimides were evaluated and compared. Those with known composition are given in Figure 1. Seven of the poly-

imides were evaluated as films (20 to 25 μm thick) applied to sandblasted AISI 440C HT (high temperature) stainless steel disks (Rockwell hardness, C-60; surface roughness, 0.9 to 1.2 μm CLA). Those polyimides are designated PIC-1 to PIC-7. Three of the polyimides were evaluated as solid bodies or composites; they are designated Types "A", "C", and "V". The polyimide film PIC-7 and the polyimide solid body Type "C" are the same polyimide. Polyimide Type "V" is a common commercially available polyimide.

Polyimide-bonded solid lubricant films were formulated using the PIC-1 polyimide and 75 weight percent of molybdenum disulfide (MoS_2) or 50 weight percent of graphite fluoride ($(CF_{1.1})_n$). One commercially available composite containing 15% graphite powder in a Type "V" polyimide matrix was also evaluated. Graphite fiber reinforced composites (GFRPI) were made from 50 weight percent low modulus graphite fibers and Type "A" polyimide. The fibers were 8.4×10^{-6} meter in diameter and chopped into lengths of 6.4×10^{-3} meter. They were randomly dispersed throughout the polyimide matrix. For more details on the films or composites see references 20 to 29.

The hemispherically tipped pins were made of AISI 440C HT stainless steel or the polyimide composite material. The 440C pins were slid against the polyimide films or composite disks and the composite pins were slid against smooth 440C disks with a surface roughness of less than 0.1 μm, CLA.

EXPERIMENTAL PROCEDURE

A pin-on-disk tribometer was used for these experiments (Figure 2). The pins were either hemispherically tipped with a radius of 0.475 cm or the same hemispherically tipped pins with flats worn on them (see insert, Figure 2). They were loaded with a 9.8 N deadweight against the disk which was rotated at 1000 rpm. The pin slid on the disk at a radius of 2.5 cm giving it a linear sliding speed of 2.7 m/s. The test specimens were enclosed in a chamber so that the atmosphere could be controlled. Atmospheres of dry argon (ë100 ppm H_2O), dry air (ë100 ppm H_2O), or moist air (10 000 ppm H_2O) were evaluated.

Each test was stopped after predetermined intervals of sliding and the pin and disk were removed from the friction apparatus. The contact areas were examined by optical microscopy and photographed, and surface profiles of the disk wear track were taken. Locating pins insured that the specimens were returned to their original positions. Disk wear was determined by measuring the cross-sectional area on the disk wear track (from surface profiles), and rider wear was determined by measuring the wear scar diameter on the hemispherically tipped rider after each sliding interval and then calculating the volume of material worn away.

RESULTS AND DISCUSSION

Polyimide Films

General wear mechanisms. The wear process of a polyimide solid body or a composite body is one of gradual wear through that body[20]. A film, however, can wear and lubricate by either of two processes[21-22]. One, it can wear similar to a solid body by gradually wearing away; or two, it can be quickly worn away with the subsequent formation of a secondary film at the substrate interface. In the second mechanism, shearing of the secondary film provides the lubrication. Figure 3 gives cross-sectional views of a film wear track, illustrating these two mechanisms.

When gradual wear through the film occurs, generally no measurable wear occurs to the metallic pin; but when the lubrication process is of the secondary film type, wear of the rider increases usually at a constant rate with sliding distance. This is most probably due to the fact that some metal to metal contact occurs during the shearing of the film.

All seven polyimide films evaluated could provide lubrication by either mechanism[22]. In general, the rider wore gradually through the film and then a secondary film formed which provided lubrication for an extended period of time. The secondary film mechanism for the polyimide films was not studied in great detail since lubrication by this mechanism is usually improved by the addition of a solid lubricant such as graphite or graphite fluoride. Also, if possible, the gradual wear through film mechanism is preferred, since there is less chance of adhesive metal to metal wear occurring which could lead to catastrophic failure.

Friction and wear - 25° C. Polyimide film wear volume tended to increase in a linear manner (from zero) as a function of sliding distance. Figure 4 plots wear volume for a representative polyimide film as a function of sliding distance. Wear rates were determined by taking a linear regression fit (least squares) of these data. Average wear rates are given for each polyimide evaluated in Table I.

The table also gives the average "steady state" friction coefficient obtained for each polyimide. The table indicates that the three films that gave the lowest friction coefficients also gave the highest wear rates. The other four films gave higher friction coefficients but lower wear rates.

The polyimide films were thus classified into two groups[22]: Group I, low friction coefficients (<.13) - high wear rates (>40 x 10^{-14} m^3/m) and Group II, high friction coefficients (>.23) - low wear rates (<12 x 10^{-12} m^3/m).

Film wear surface morphology - 25° C. The polyimides were classified into the two groups not only because of their friction

and wear properties, but because of similarities in film wear track surface morphology. Representative photomicrographs of each group are shown in Figures 5 and 6.

Group I wear surfaces were characterized by being covered with powdery, agglomerated, birefringent polyimide wear particles. The wear process was of an adhesive nature; but the surface layer appeared to be brittle and subsequent crumbling of it into relatively large particles readily occurred. Transfer to the pin was found to be thin and tended to plastically flow across the contact area.

Group II polyimides were characterized by a rough looking surface (Figure 6) that tended to plastically flow for a short distance, but then tended to break-up into very fine wear particles at the leading edge. The wear particles did not agglomerate on the film wear track as did Group I polyimides, although they had a tendency to build-up on the metallic pin.

One polyimide in Group II (PIC-2) produced wear surfaces that had only localized rough looking areas (Figure 7). For this polyimide, the wear surface, in general, was very smooth with striations in the sliding direction. But, even though these surfaces were smoother than other Group II polyimides, film wear rates and friction coefficients were not significantly different.

From a surface morphological point of view, however, PIC-2 films produced the most desirable wear tracks, a smooth, almost glass-like wear surface (Figure 7). Also the transfer films tended to be thinner and to coalesce and plastically flow across the pin contact area better than the other Group II polyimides. The other polyimides tended to form transfer films of compacted polyimide wear particles which slid across the metallic pin and tended to wear it.

Molecular relaxations. It is well known that most polymers have a glass-transition temperature (T_G) which marks their change from a rubbery state to a glassy state. It is not so well known that polymers also possess secondary transitions below their T_G. Some of these secondary transitions appear to influence the mechanical properties of polymers.

Both the glass transition and the secondary transitions can be related to one or more molecular relaxation processes (changes in motion within polymer chains). The glass transition is related to the motion of longer segments of the main chain; while the secondary transitions are related to rotations or oscillations of side chains, subgroups, chain ends or short segments of the main chain.

The friction and wear properties of the polyimide film PIC-1 have been compared to the molecular relaxations that occur in this polyimide[23]. Figure 8 gives this comparison, where the logarithmic decrement (from torsional braid analysis (TBA)) and

friction coefficient (obtained in dry argon) are plotted as a function of temperature for a film cured in air and for the same film heated to 500° C in dry argon.

The peaks in the logarithmic decrement curve (α, β, β_{H_2O}, γ) represent loss maxima or temperatures at which the molecular segment achieves its greatest degree of freedom. As the temperature is decreased below the loss maxima, the motion responsible for the loss mechanism is continuously hindered, until at some temperature it becomes completely frozen. This is the onset temperature of the peak.

A large transition in the friction coefficient of PIC-1 polyimide films occurred at approximately 30° to 40° (Figure 8). If the secondary molecular relaxation were responsible for this transition, it appears the onset of the peak rather than the peak maxima is the parameter which best correlates to the friction transition.

Figure 8 also indicates that, by heating the polyimide in dry argon to 500° C, the T_G of the polyimide was increased to that temperature, with the subsequent reduction in friction coefficient between the tempertures of 300° and 500° C.

Temperature and atmosphere effects. In addition to temperature, atmosphere can also markedly affect the friction and film wear properties of polyimide films[24]. Figure 9 plots average friction coefficient and film wear rate as a function of temperature for PIC-1 polyimide films evaluated in these different atmospheres; dry argon (<100 ppm H_2O), dry air (<100 ppm H_2O) and moist air (10 000 ppm H_2O).

In dry air and argon, a transition (from higher friction and wear to lower friction and wear) occurred between the temperatures of 25°C and 100° C. But in moist air, this transition has shifted to a higher temperature. It has been postulated that this shift in transition temperature in moist air is due to the β_{H_2O} molecular relaxation (Figure 8). The H_2O molecules are believed to hydrogen bond to the polyimide molecules, constraining their motion, and inhibiting their ability to plastically flow in thin surface layers.

Figure 10 gives a typical film wear surface for temperatures above the transition. The wear track becomes very smooth and the primary wear mechanism appears to be the spalling of a thin, textured layer of the polyimide (Figure 10). Similarly, the transfer films tend to flow across the pin in very thin layers and there is no tendency for them to buildup with sliding duration as they did at 25° C.

At temperatures below the transition, atmosphere did not markedly affect film wear rate (Figure 9), but H_2O in the

atmosphere did tend to reduce the friction coefficient at this temperature. At temperatures above the transition, lower friction and wear were obtained in argon atmospheres than in air atmospheres, indicating there may be an oxidation effect at elevated temperatures.

Polyimide - Bonded Solid Lubricant Films

High contact stress effects. Solid lubricants are often added to polymer films to improve the friction and wear characteristics; but their presence can reduce the load carrying capacity of the polymer. In reference 25, molybdenum disulfide (MoS_2) and graphite fluoride ($(CF_{1.1})_n$) were added to PIC-1 polyimide films. The presence of the solid lubricants reduced the strength of the films to the point that they would not support the hemispherical-tipped pin sliding under a load of 9.8 N.

Figure 11 illustrates what happened to the polyimide-bonded $(CF_{1.1})_n$ film under the above sliding conditions[21]. A series of fine cracks developed on the film wear track which led to the eventual crumbling away of the film in less than 15 kilocycles of sliding. Once this took place, lubrication occurred by the secondary film mechanism. Polyimide and $(CF_{1.1})_n$ wear debris compacted into valleys between sandblasted asperties in the 440C stainless steel disk substrate, and flat plateaus were worn in the asperities (Figure 11(b)).

The mechanism of lubrication became the process of shearing very thin films of the polyimide - $(CF_{1.1})_n$ mixture between flat areas on the pin and on the metallic asperities. This process continued until the lubricant became depleted from the valleys.

Figure 12 plots wear life (defined as the number of sliding revolutions to reach a friction coefficient of 0.30) and average friction coefficient as a function of temperature for polyimide alone and for polymide-bonded $(CF_{1.1})_n$ or MoS_2 films.

MoS_2 tended to improve the friction characteristics of polyimide to temperatures of 400° C, and the wear life at 25° C; but at 100° C and higher, shorter, wear lives were obtained. $(CF_{1.1})_n$ improved the wear life at all temperatures but only improved the friction coefficient at 25° C. Of course, one must realize that a different wear process (gradual wear through film) occurred for polyimide by itself at temperatures of 100° C and higher.

Low contact stress effects. It was discovered in reference 21, that if lower contact stresses were applied to the polyimide-bonded $(CF_{1.1})_n$ films, the bonded film itself could support the load and the film would wear in a manner similar to polyimide alone. Figure 13 shows a photomicrograph on a polyimide-bonded graphite fluoride film subjected to a projected contact stress of 14 MPa.

The figure illustrates the tips of the film asperities can support this load. Wear at this point is a process of gradual truncation of these asperities.

Two general wear processes were observed to occur. One was the spallation of a very thin textured layer (<1μm) of the film (Figure 14(a)) and the other was the brittle fracture of thicker surface layers (1 to 6 μm) of the film (Figure 14(b)). The occurrence of the brittle fracture wear was dependent on the contact stress, the contact area, and the build-up of thick transfer films[26]. Low contact stresses and large contact areas tended to promote the build-up of thick, non-flowing transfer films which increased adhesion and thus friction and wear.

Figure 15 gives a friction trace for a 0.95-mm diameter flat sliding against a 45-mm-thick polyimide-bonded film. The trace is divided into two regions: the first stage of lubrication where gradual wear through the film occurs and the second stage of lubrication where the lubrication occurs by the secondary film. In the first stage of lubrication, friction tends to increase gradually with sliding duration. This increase corresponds to truncation in the film asperities and the ensuing increasing contact area. Once full contact was obtained, the average friction coefficient during the first and second stages of lubrication were nearly equivalent (0.24).

Polyimide Solid Bodies

Friction and wear. In addition to use as films, polyimides have also been molded into solid bodies and their tribological properties evaluated[20]. Figure 16 compares average friction coefficients and wear rates at 25° C for 440C HT stainless steel hemispherically tipped pins sliding on two different polyimide solid bodies made from types "A" and "V" polyimides. In addition, the figure shows similar data for composites made by adding 15% graphite powder to type "V" polyimide and by adding 50% graphite fibers to type "A" polyimide.

The friction coefficients of both polyimides are rather high compared to the polyimide films, but the wear rate of type "A" polyimide fits in very well with Group II polyimide films (Table I). Additions of 15% graphite powder to type "V" polyimide reduced the friction coefficient but the wear rate (at least with this geometry) remained the same as the base polyimide (Figure 16). Additions of 50% graphite fibers to type "A" polyimide markedly improved the friction coefficient (0.40 to 0.19) and the wear rate (35×10^{-14} to 0.6×10^{-14} m^3/m) when compared to the base polyimide.

The graphite fiber reinforced polyimide (GFRPI) was also evaluated at 300° C. Friction coefficient was even lower at this temperature (0.05) but the wear rate was nearly the same (0.7×10^{-14} m^3/m) as at 25° C.

Wear mechanisms. A photomicrograph of typical wear surface morphology at 25° C on type "A" polyimide solid bodies is shown in Figure 17. The wear surface was rough looking and consisted of thick plastically flowing surface layers (up to 3μm) that tended to spall and crumble. Even though wear rates were higher (Figure 16) and wear mechanisms different, friction coefficients and transfer films were similar to Group II polyimide films. That is, thick, non-shearing transfer films tended to build-up with increasing sliding duration.

Type "V" polyimide tended to wear similar to Group II polyimide films (Figures 6 and 7). The addition of 15% graphite powder did not markedly alter the wear process. Figure 18 gives a typical photomicrograph of the wear surface of 25° C on this composite. The graphite particles did not mix with the polyimide to form a surface layer; and in fact may have weakened the structure slightly, since pits and crumbling was observed on the wear surface (Figure 18).

Figure 19 gives a photomicrograph of a typical wear track surface in moist air for a low modulus graphite fiber reinforced polyimide composite. The fibers have mixed together with the polyimide to form a very thin surface layer. The wear process appears to be the spalling of this surface layer (Figure 29).

At 300° C, the fibers did not mix with the polyimide on the wear surface as they did at 25° C (Figure 20). Instead a very thin layer of the polyimide tended to flow across the fibers and dominate the friction process. As mentioned in a previous section, some polyimides possess transitions, above which very low friction occurs.

Geometry effects. In reference 27, the sliding specimen configuration was reversed and a hemispherically tipped GFRPI composite pin was slid against a 440C HT stainless steel disk counterface. The friction coefficients and composite wear rates were found to be highly dependent on sliding duration. Initial friction coefficients were slightly lower than those obtained on composite disks (0.15 vs 0.19) but as sliding duration increased, the friction coefficient rose to an average value of 0.27 or higher.

Average composite pin wear rates were initially (up to 20 km of sliding) lower than composite disk wear rates (2.5×10^{-15} m^3/m vs 13×10^{-15} m^3/m); but as sliding duration increased pin composite wear rate increased and after 19 km of sliding, composite pin wear rate was 41×10^{-15} m^3/m.

The reasons for these differences can be inferred from differences in wear surface morphology for a GFRPI pin sliding against a 440C HT disk after long sliding durations. Initially transfer films to the disk were very thin (similar to the opposite configuration), but as sliding duration increased, thick, non-shearing

transfer occurred (Figure 21(b)) which increased both friction and wear. There was considerable back transfer to the composite pin (Figure 21(a)), and the fibers and polyimide did not mix together to form a shear film as was the case for the opposite configuration.

The friction and wear data from pin-on-disk tests has been compared to data from an end use application, plain spherical bearing (Table II)[28-29]. It is interesting to note that results from the bearing tests compare very closely to the pin-on-disk tests when the metal pin slid against the GFRPI composite, but not when a composite pin slid against the metal counterface. These observations point out the importance of evaluating materials in a configuration that closely approximates the intended end use application.

Comparison to Other Polymers

The friction and wear properties of polyimide films, solid bodies, and composites are compared to some commercially available polymers in Table III. All were evaluated at Lewis Research Center under the same experimental conditions on a pin-on-disk tribometer.

Except for Ultra-High-Molecular-Weight Polyethylene (UHMWPE), the polyimide formulations are much superior to the others. UHMWPE is a material currently being used in artificial human joints[30]. It is an exceptionally good friction and wear material at ambient temperatures (25° C), but does not have high temperature stability.

The best polyimide material (under high stresses) at 25° C was GFRPI. It had a higher friction coefficient than UHMWPE (0.19 vs 0.13) but wear rate was lower (130×10^{-16} vs 380×10^{16} m^3/m). At 300° C, approximately the same wear rate for GFRPI was obtained, and the friction coefficient was much lower (0.05).

The best friction and wear properties (of any polymer) were obtained with the PIC-1 polyimide film at 100° C in dry argon. A friction coefficient of 0.02 and a wear rate of 8×10^{-16} m^3/m was obtained. Low wear rates were also obtained with PIC-1 polyimide-bonded graphite fluoride films at 25° C under low contact stresses (30×10^{-16} m^3/m).

CONCLUDING REMARKS

The tribological properties of polyimide films, polyimide solid bodies, polyimide-bonded solid lubricant films, and polyimide composites have been discussed and compared. The results indicate they have considerable promise for self-lubricating applications to temperatures of 350° C in air, however the upper temperature limit is dependent on which type of polyimide is used and the nature of the application.

In general, the polyimides tend to be brittle and wear by the brittle fracture of surface layers (up to 3μm or more, depending upon the contact stresses applied). To obtain optimum lubrication with the polyimides it is believed that shear must be induced to occur in very thin surface layers (<1μm).

Some polyimides possess a transition temperature, above which the molecules obtain a degree of freedom necessary to plastically flow in these thin layers; but H_2O molecules from the atmosphere can hydrogen bond to the molecular chains and constrain their motion. That is, the transition is either masked in the presence of water vapor or translated to a higher temperature.

Thus, the tribological problem is altering the polyimide in some manner to induce the formation of thin surface layers at temperatures below the transition. The addition of solid lubricants can help in this, but the solid lubricant must be compatible with the polyimide in order that they mix together to form the very thin surface layers. In that regard, graphite fluoride ($(CF_x)_n$) works well with polyimide in that the two mix together and shear in a very thin surface layer under light contact stresses. A disadvantage of adding powdered solid lubricants (such as ($(CF_x)_n$)) is that they tend to reduce the load carrying capacity of the film or composite, since they tend to agglomerate and have planes of easy shear.

Graphite fibers can be added to polyimide solids to increase the load carrying capacity by reinforcing the structure. In addition they can improve the friction and wear properties. Graphite fibers tend to dominate the tribological results, and different types of fibers can produce different results.

Polyimides, with or without solid lubricant additions, tend to produce thick, non-shearing transfer films which lead to increased friction and wear. It is believed this problem can be mitigated by proper additive formulation or by the proper sliding configuration design. Smaller contact areas and higher contact stresses tend to produce thinner transfer films.

REFERENCES

1. N. W. Todd and F. A. Wolff, Mater. Des. Eng., 60 (2), 86-91 (1964).
2. C. E. Sroog, A. L. Endrey, S. V. Abramo, C. E. Berr, K. L. Olivier, and W. M. Edwards, J. Polym. Sci., Pt. A., 3 (4), 1373-1390 (1965).
3. J. F. Hencock and C. E. Berr, SPE Trans., 5 (2), 105-110 (1965).
4. N. A. Adrova, M. I. Bessonov, L. A. Laius, and A. P. Rudakov, "Polyimides: A New Class of Thermally Stable Polymers," Progress in Materials Science Series, 7, Technomic Publishing Co., Inc., Stamford, Conn., 1970.

5. R. L. Fusaro, NASA TM-81381, 1980.
6. J. K. Lancaster, Tribology, 6 (6), 219-251 (1973).
7. F. J. Hermanek, Met. Prog. 97 (3), 104-106 (1970).
8. J. Theberge, in "ASLE Proceedings - International Conference on Solid Lubrication," SP-3, pp. 166-184, American Society of Lubrication Engineers, Park Ridge, Ill., 1971.
9. R. D. Brown and W. R. Blackstone, in "Composite Materials; Testing and Design," ASTM STP-546, pp. 457-476, American Society for Testing and Materials, Philadelphia, PA., 1974.
10. H. E. Sliney and R. L. Johnson, NASA TN D-7078, 1972.
11. S. Bangs, Power Transm. Des., 15 (2), 27-31 (1973)
12. M. N. Gardos and B. D. McConnel, ASLE Preprint No. 81-LC-3A-3, 1981.
13. J. P. Giltrow and J. K. Lancaster, in "International Conference on Carbon Fibres, Their Composites and Applications," Paper 31, Plastics Institute, London, 1971.
14. J. P. Giltrow and J. K. Lancaster, Nature, 214 (5093), 1106-1107 (1967).
15. J. K. Lancaster, J. Phys. D., 1, 549-559 (1968).
16. R. A. Simon and S. P. Prosen, in "Twenty-Third Annual Technical Conference, SPI Reinforced Plastics Composite Division, Proceedings," Section 16-B, pp. 1-10, Society of the Plastics Industry, Inc., New York, 1968.
17. J. W. Herrick, in "Reinforced Plastics-Ever New; Proceedings of the Twenty-Eighth Annual Technical Conference," pp. 17-D1 to 17-D6, Society of the Plastics Industry, Inc., New York, 1973.
18. J. P. Giltrow and J. K. Lancaster, in "Tribology Convention, Pithochry, Scotland, May 15-17, 1968, Proceedings," pp. 149-159, Institution of Mechanical Engineers, London, 1968.
19. M. N. Gardos and B. D. McConnell, ASLE Preprint No. 81-LC-3A-4, 1981.
20. R. L. Fusaro and H. E. Sliney, ASLE Trans., 21 (4) 337-343 (1978).
21. R. L. Fusaro, ASLE Trans. 24 (2), 191-204 (1981).
22. R. L. Fusaro, NASA TP-1944, 1982
23. R. L. Fusaro, ASLE Trans., 20 (1), 1-14 (1977).
24. R. L. Fusaro, ASLE Trans., 21 (2), 125-133 (1978).
25. R. L. Fusaro, NASA TN D-6714, 1972.
26. R. L. Fusaro, Wear, 75, 403-422 (1982)
27. R. L. Fusaro, ASLE Preprint 82-AM-5A-2, 1982.
28. H. E. Sliney and T. P. Jacobson, NASA TP-1229, 1978.
29. H. E. Sliney, Lubr. Eng., 35 (9) 497-502 (1979).
30. D. A. Sonstegard, L. S. Matthews, and H. Kaufer, Sci. Am., 238 (1) 44-51 (1978).

Table I. - Classification of Polyimide Films into Two Friction and Wear Groups, for Ambient Temperature Conditions (22° to 27° C in 50% R.H. air).

Polyimide Type	Average "Steady State" Friction Coefficient	Average Film Wear Rate	Group
PIC - 1	0.13	40×10^{14} m^3/m	
PIC - 4	0.13	80×10^{-14} m^3/m	I
PIC - 7	0.10	40×10^{-14} m^3/m	
PIC - 2	0.23	10×10^{-14} m^3/m	
PIC - 3	0.27	6×10^{-14} m^3/m	II
PIC - 5	0.30	6×10^{-14} m^3/m	
PIC - 6	0.28	12×10^{-14} m^3/m	

Table II. Comparison of Friction and Wear Data Obtained on GFRPI Composites Using Different Experimental Apparatus and Geometries

Experimental Apparatus	Composite Wear Specimen	Temperature, °C	Average Friction Coefficient	Average Wear Rate, m^3/m
Self-aligning plain bearings	Molded liner	25	0.15	1.2×10^{-14}
		315	0.05	1.2×10^{-14}
	Insert liner	25	0.15	2.0×10^{-14}
		315	0.05	2.0×10^{-14}
Pin-on-disk	Pin	25[a]	0.15	$.25 \times 10^{-14}$
		25[b]	0.27	4.1×10^{-14}
		300[a]	0.50	20×10^{-14}
	Disk	25	0.19	1.3×10^{-14}
		300	0.05	1.5×10^{-14}

(a) Sliding distance of 1 km
(b) Sliding distance of 19 km

Table III. - Comparison of Average Friction Coefficients and Wear Rates of Some Commercially Available Materials to Polyimide Films, Solid Bodies, and Composite Materials Evaluated Under the Same Conditions.

[Pin-on-disk tribometer; hemispherically tipped pin, 440C stainless steel; films applied to 440C stainless steel disks or disks made of material evaluated; speed, 1000 rpm (2.7 m/s); load, 1 kg; controlled testing atmosphere of 50% RH air.]

Material evaluated	Temperature (C°)	Film or Solid	Average Friction Coefficient	Average Wear Rate (m^3/m)
Polyphenlene sulfide ** 40% graphite fibers	25	solid	0.30	6200×10^{-16}
Poly (amide-imides) ** PTFE & Graphite powders	25	solid	0.37	1800×10^{-16}
UHMWPE **	25	solid	0.13	380×10^{-16}
Type "A" polyimide	25	solid	0.40	3500×10^{-16}
Type "V" polyimide **	25	solid	0.54	1000×10^{-16}
Type "V" polyimide ** 15% graphite powder	25	solid	0.37	1000×10^{-16}
Type "A" polyimide 50% graphite fibers	25 300	solid solid	.19 .05	130×10^{-16} 150×10^{-16}
Type PIC-1 polyimide	25 100 200 100*	film film film film	.13 .24 .07 .02*	4000×10^{-16} 3000×10^{-16} 400×10^{-16} 8×10^{-16}*
Type PIC-3 polyimide	25	film	.27	600×10^{-16}
PIC-1 bonded graphite flouride powder ***	25	film	.22	30×10^{-16}

* Test atmosphere, dry argon (<100 ppm H_2O)
** Commercially available materials
*** Lower contact stress (7 MPa)

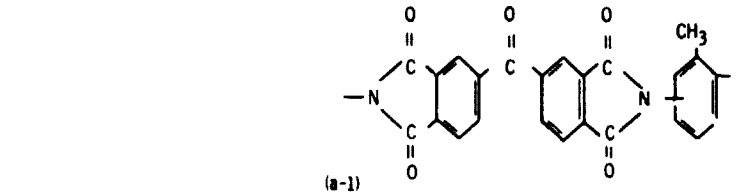

(a-1)

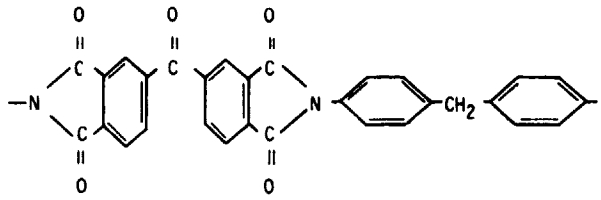

(a-2)

(a)

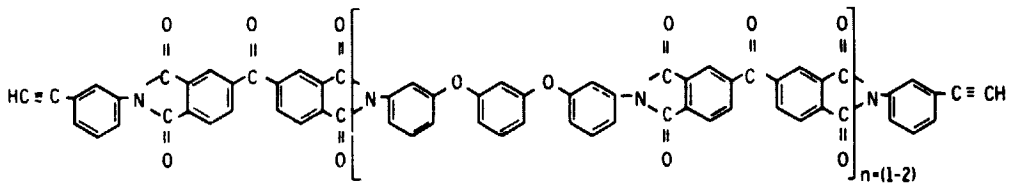

(b)

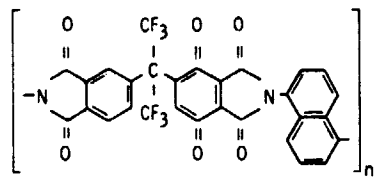

(c)

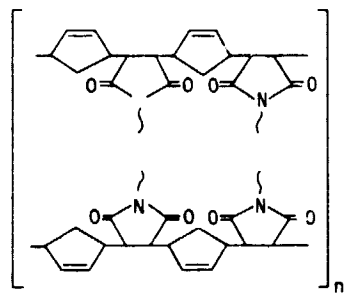

(d)

(a-1) 20 percent of the recurring units

(a-2) 80 percent of the recurring units

(a) PIC-5 polyimide film

(b) PIC-6 polyimide film

(c) PIC-7 polyimide film and type "C" solid body

(d) Type "A" idealized structure polyimide solid body

Figure 1. - Structure and designation of non-proprietary polyimides.

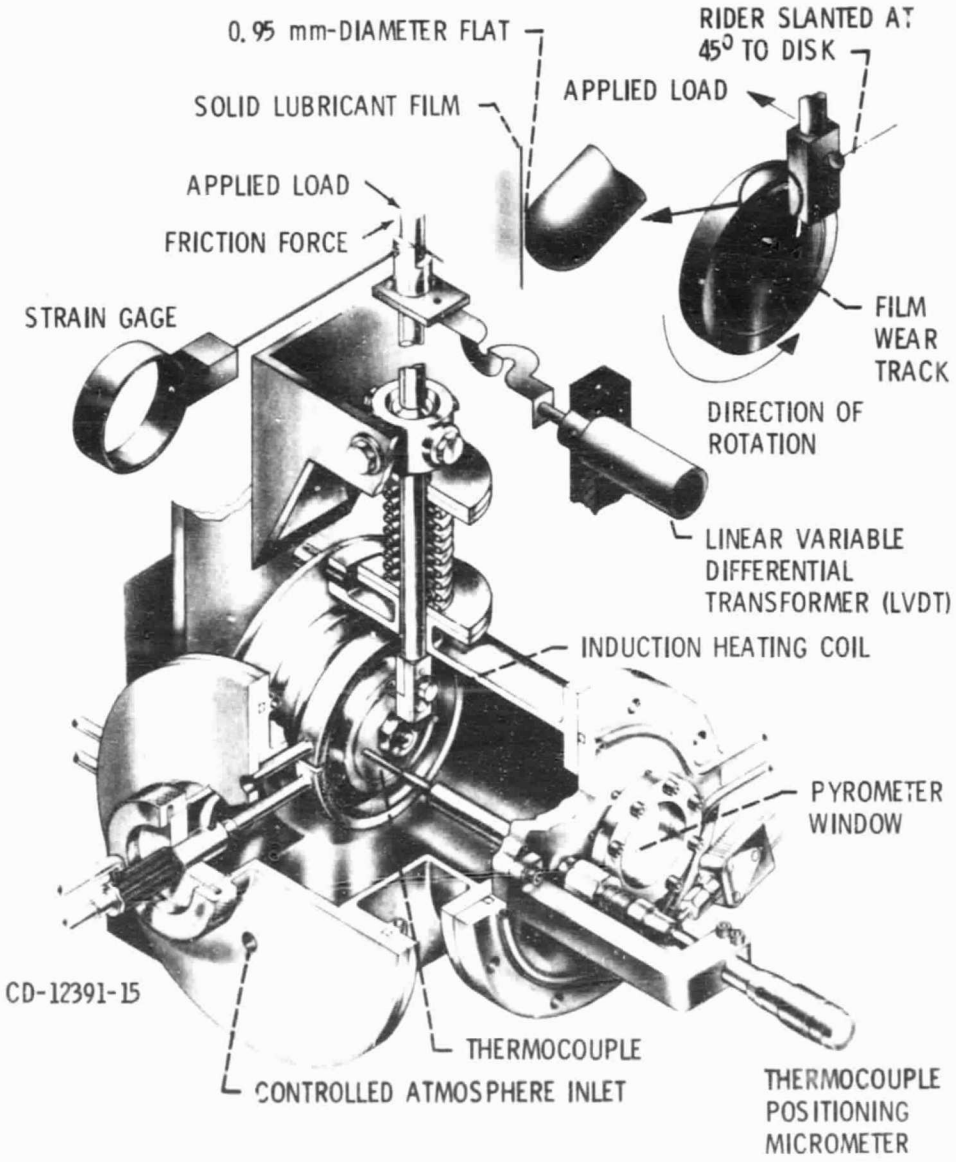

Figure 2. - Friction and wear apparatus.

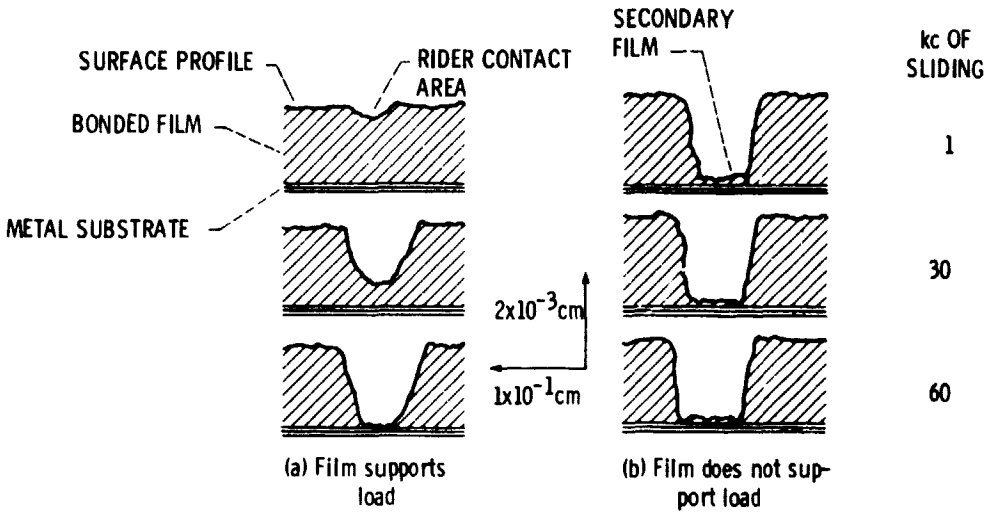

Figure 3. - Cross sectional area schematics of the wear areas on a bonded film (polymer or other type of solid lubricant film) after 1, 30, and 60 kc of sliding illustrating the two different types of macroscopic lubricating mechanisms. (Note that vertical magnification is 50 times horizontal magnification.)

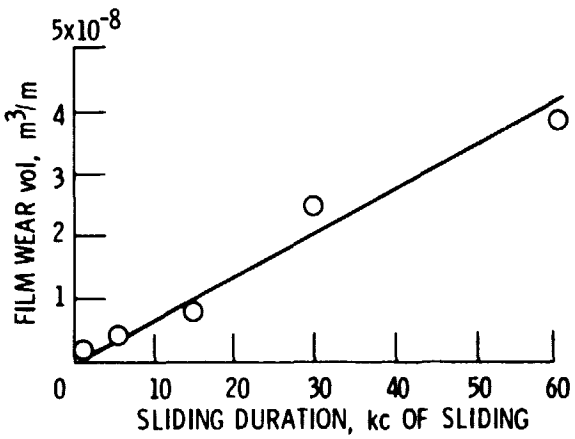

Figure 4. - Representative example of polyimide wear as a function of sliding distance. (Data from PIC-1 polyimide film at 25° C in moist air.)

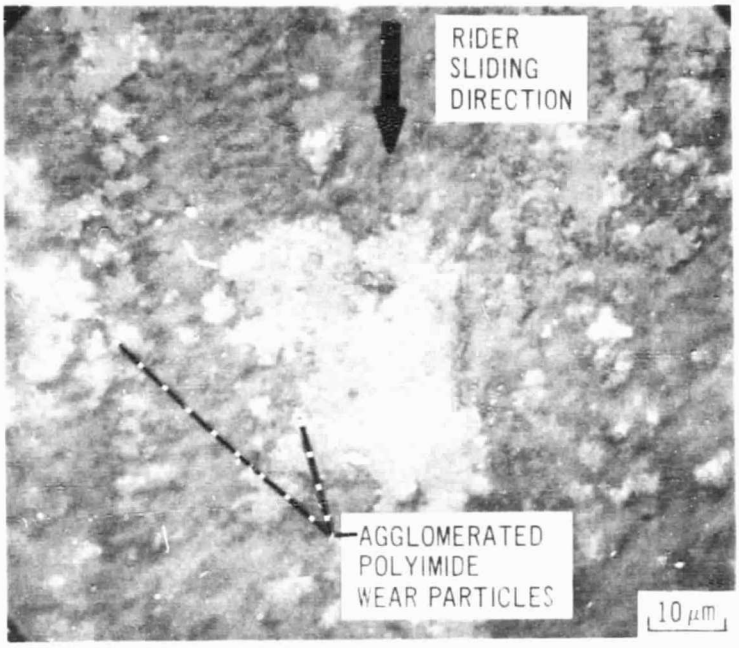

Figure 5. - High magnification photomicrograph of the wear track on PIC-4 polyimide films illustrating typical surface morphology on Group I polyimides.

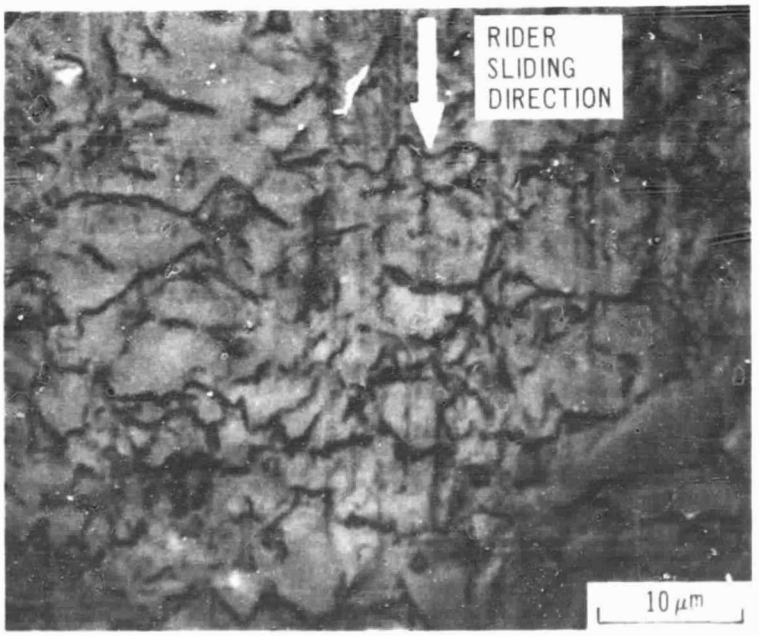

Figure 6. - High magnification photomicrograph of the wear track on PIC-3 polyimide films illustrating typical surface morphology on Group II polyimides.

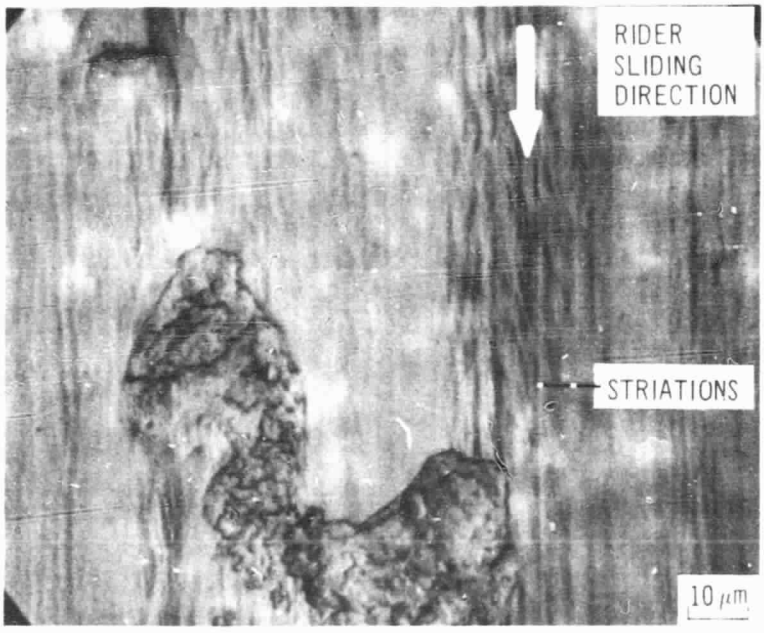

Figure 7. - High magnification photomicrograph of the wear track on PIC-2 polyimide films illustrating a variation of the wear surface morphology for Group II polyimides.

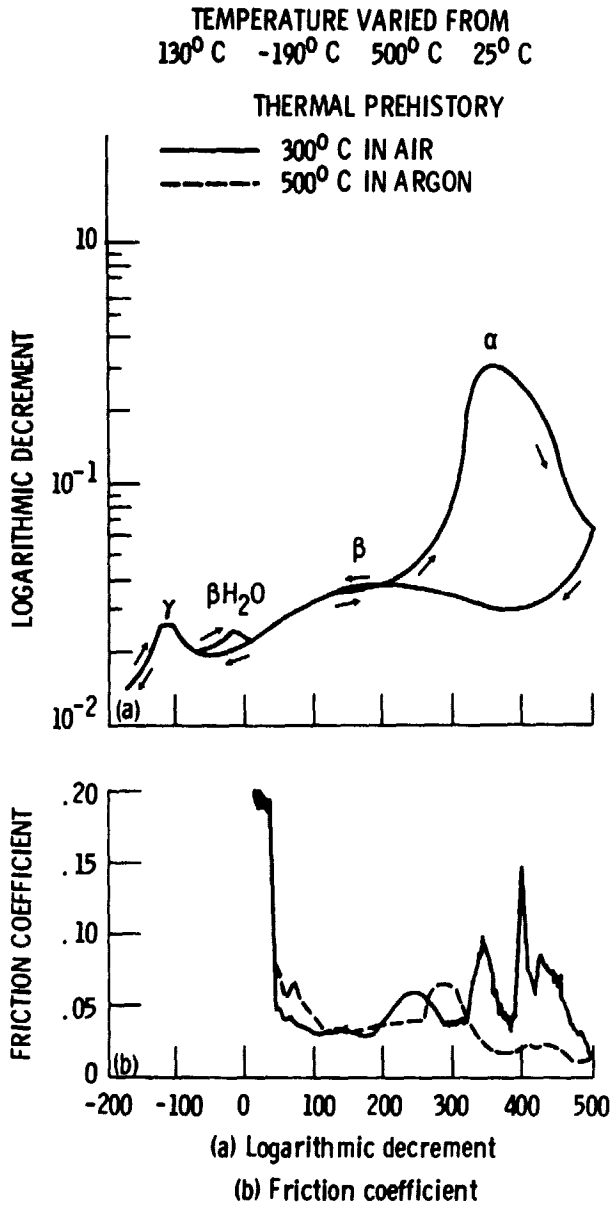

(a) Logarithmic decrement

(b) Friction coefficient

Figure 8. - Comparison of the logarithmic decrement (from torsional braid analysis) to the friction coefficient of polyimide (PIC-1) films for a film cured at 300° C in dry air and for the same film heated in argon to 500° C before testing.

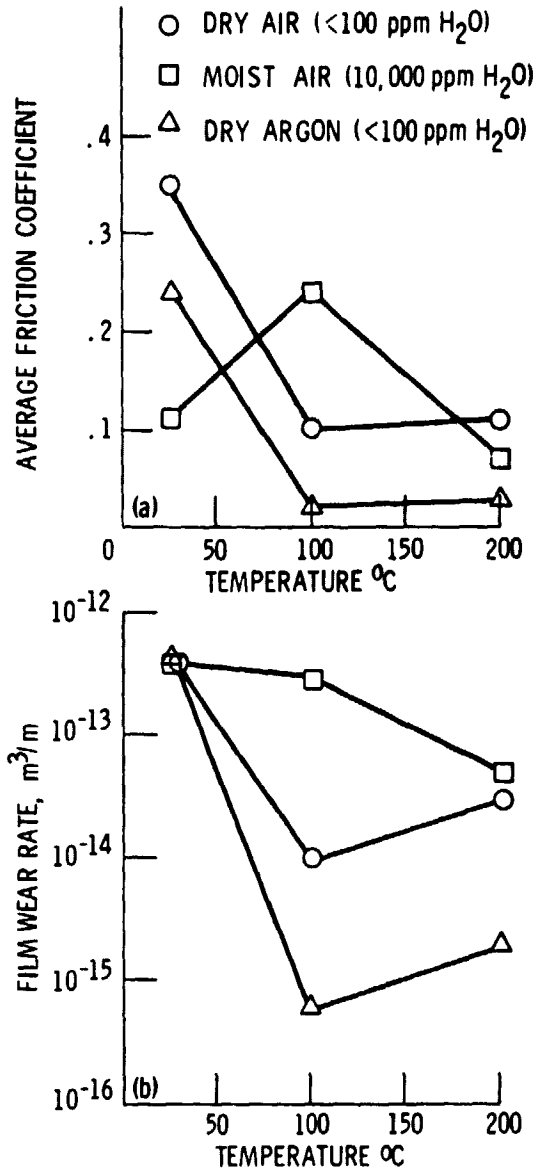

(a) Friction coefficient

(b) Film wear rate

Figure 9. - Effect of temperature and atmosphere on the friction coefficient and wear rate of polyimide films. (Specific type of polyimide film, PIC-1)

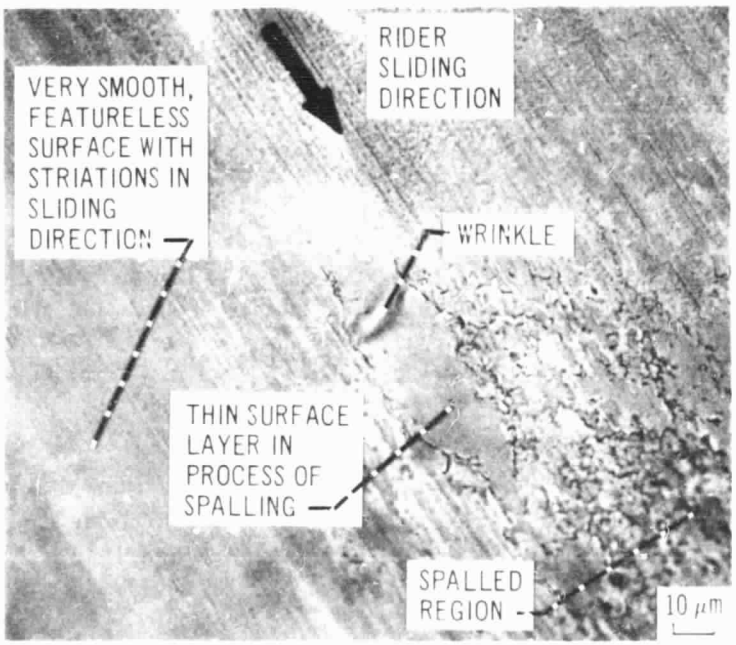

Figure 10. - High magnification photomicrograph of a PIC-1 polyimide film wear track at 150° C in dry air (< 100ppm H_2O) illustrating the sliding surface morphology at a temperature above the transition.

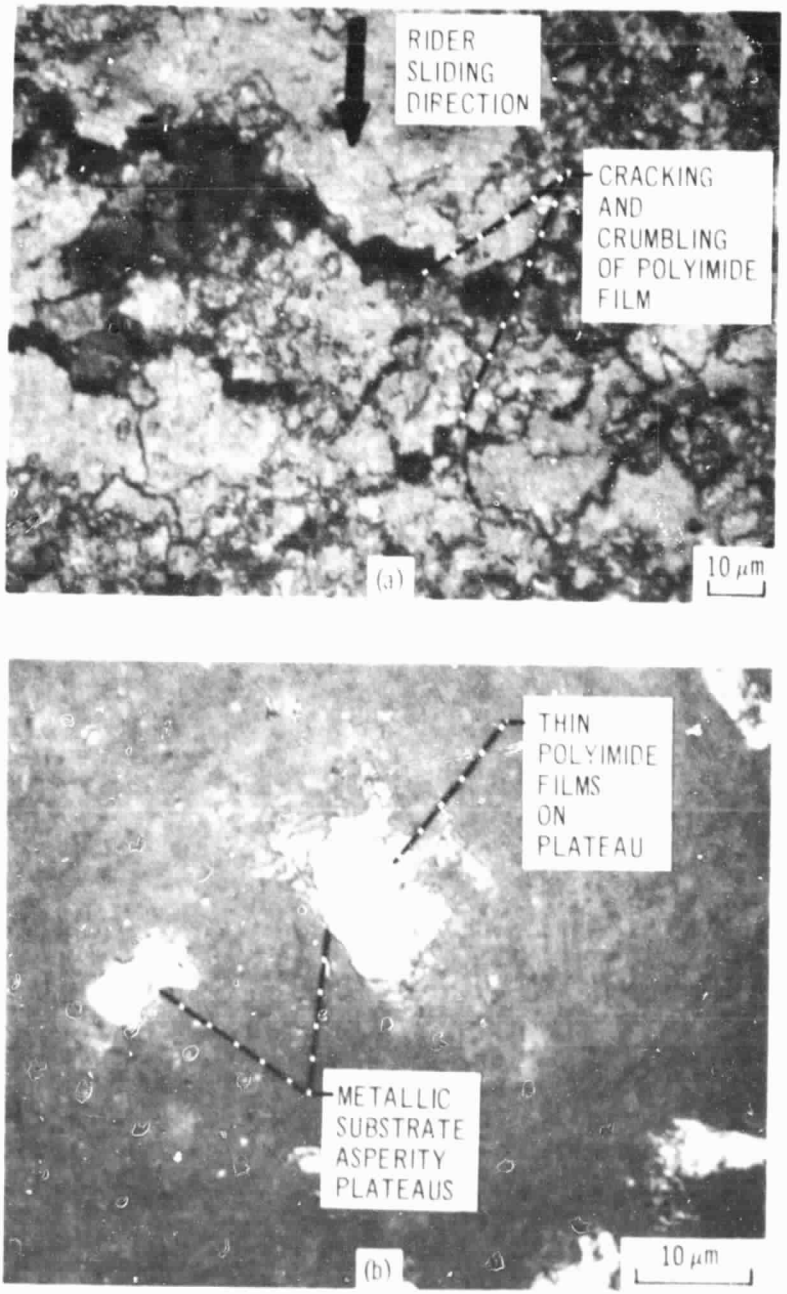

(a) Fracturing of film.

(b) Secondary film wear mechanism.

Figure 11. - Photomicrographs of wear tracks on polyimide-bonded graphite fluoride films subjected to high projected contact stress (hemisphere under 9.8 N load (stress greater than 105 MPa)).

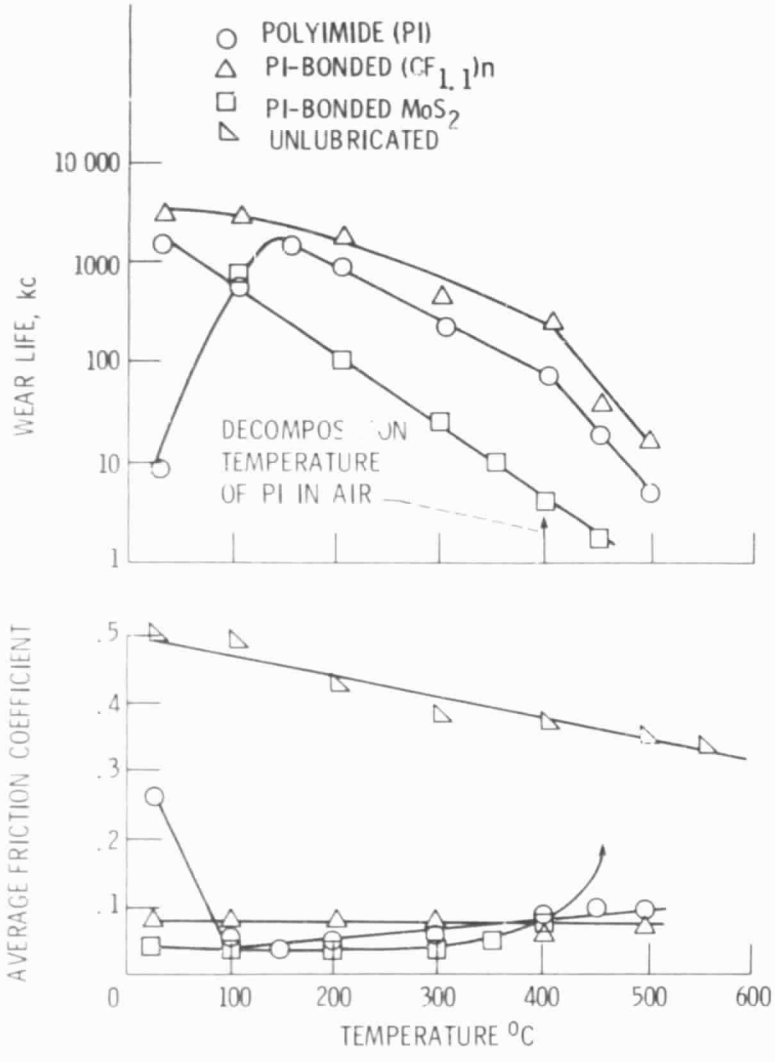

Figure 12. - Friction coefficient and wear life as a function of temperature for three solid lubricant films run in dry air (moisture content, 20 ppm).

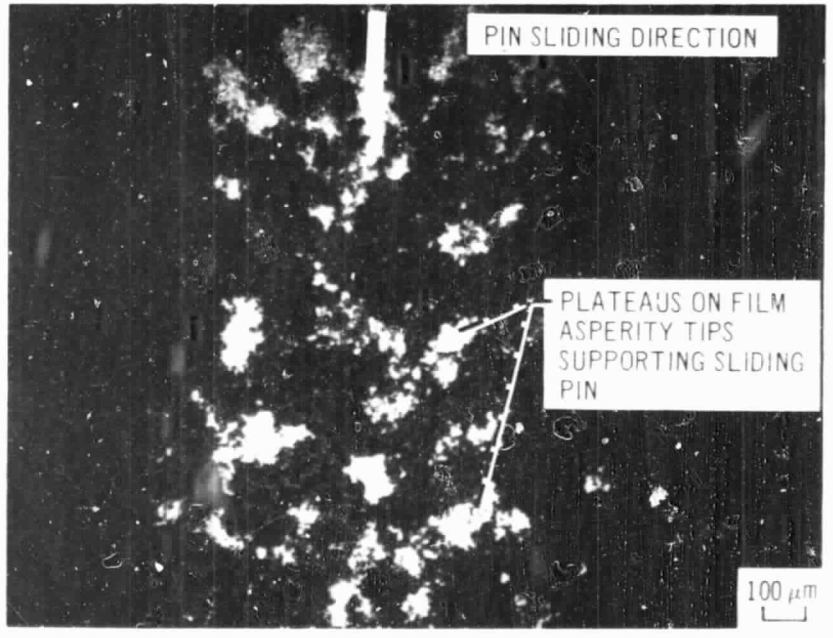

Figure 13. - Photomicrograph of wear track on polyimide-bonded graphite fluoride film subjected to a low projected contact stress (14 MPa).

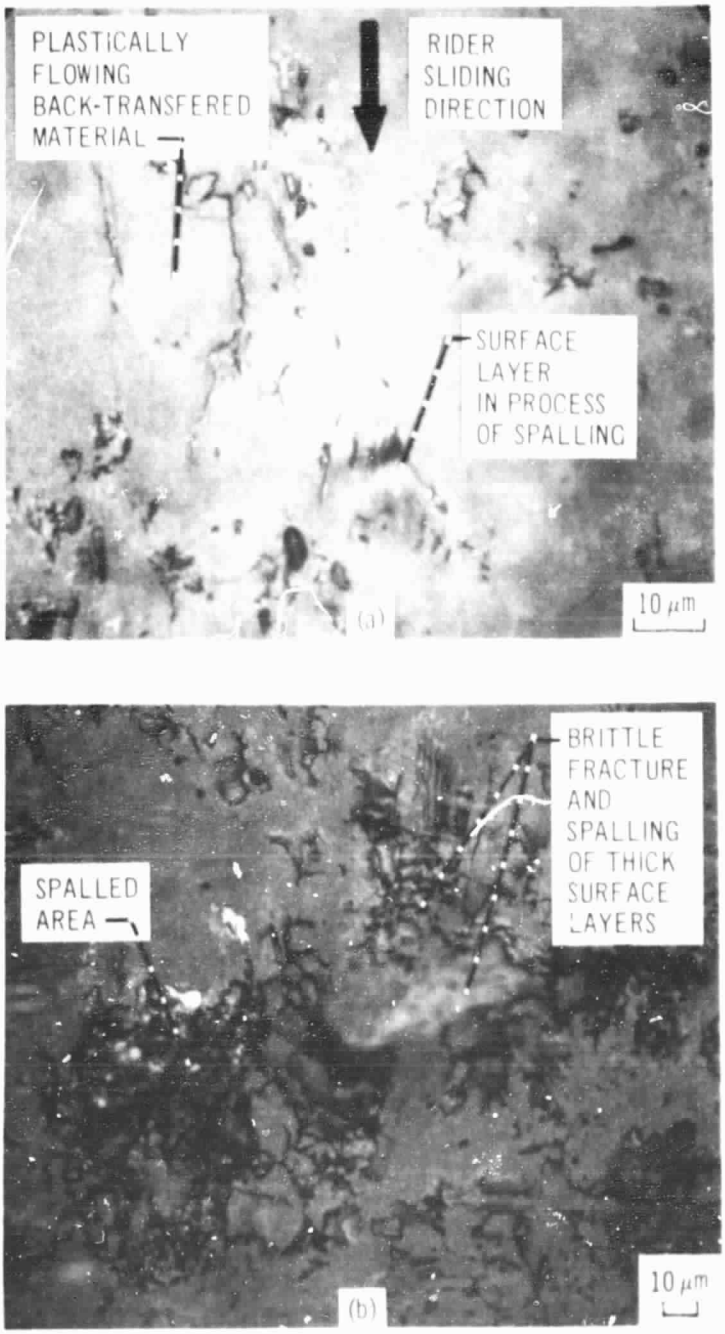

(a) Scaling of thin surface layers.

(b) Brittle fracture of thick surface layers.

Figure 14. - Photomicrographs of surface morphology on the wear tracks of polyimide-bonded graphite fluoride films subjected to low contact stresses (14 MPa) illustrating wear mechanisms.

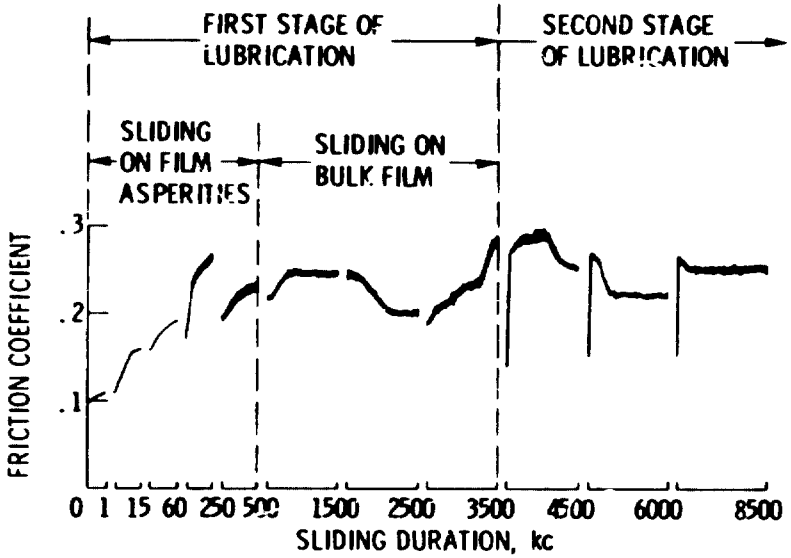

Figure 15. - Friction trace for a 440C HT stainless-steel hemispherically tipped rider (with a 0.95 mm diameter flat on it) sliding on polyimide-bonded graphite fluoride film.

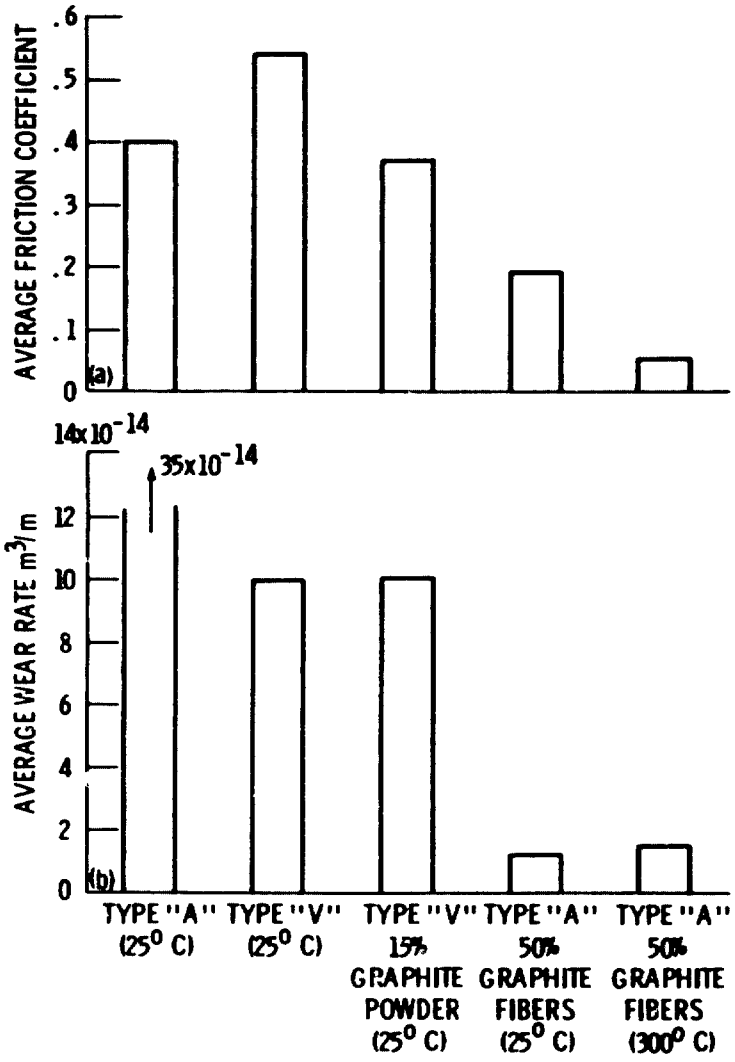

(a) Average friction coefficient

(b) Average wear rate

Figure 16. - Comparison of average friction coefficients and average wear rates of two different types of polyimides made into solid bodies (disks) and of two composite solid bodies made from the polyimides.

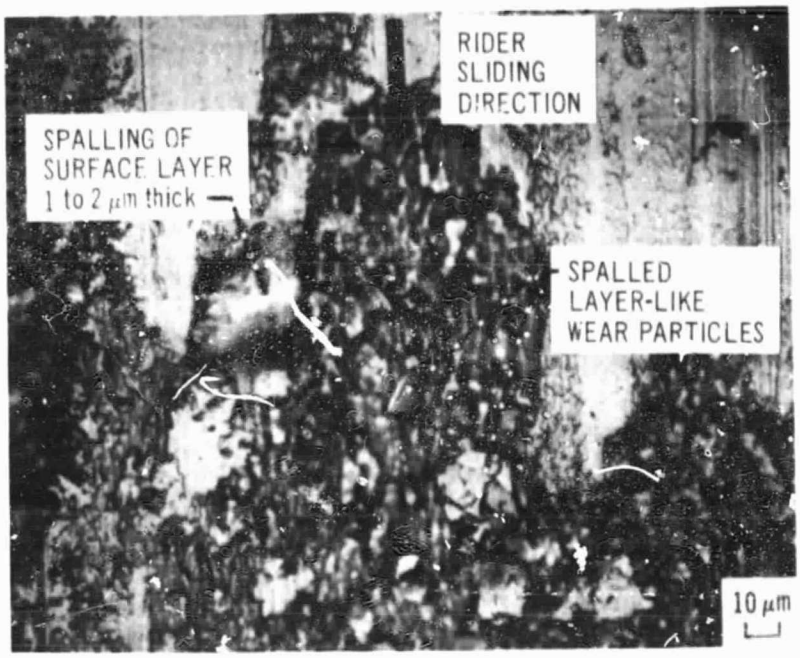

Figure 17. - Photomicrograph of typical wear surface morphology at 25° C on the type "A" polyimide solid body.

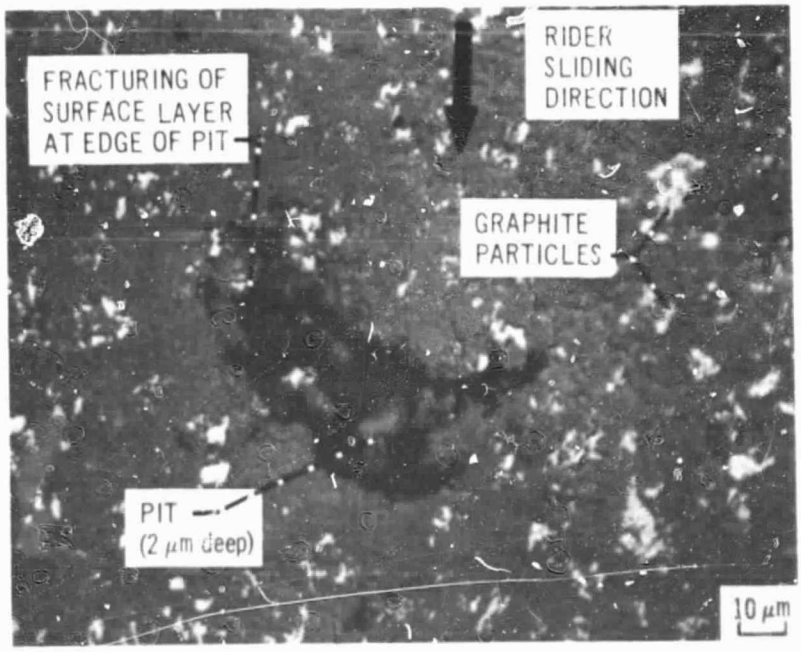

Figure 18. - Photomicrograph of typical wear surface morphology at 25° C on type "V" polyimide composites with 15% graphite powder additions.

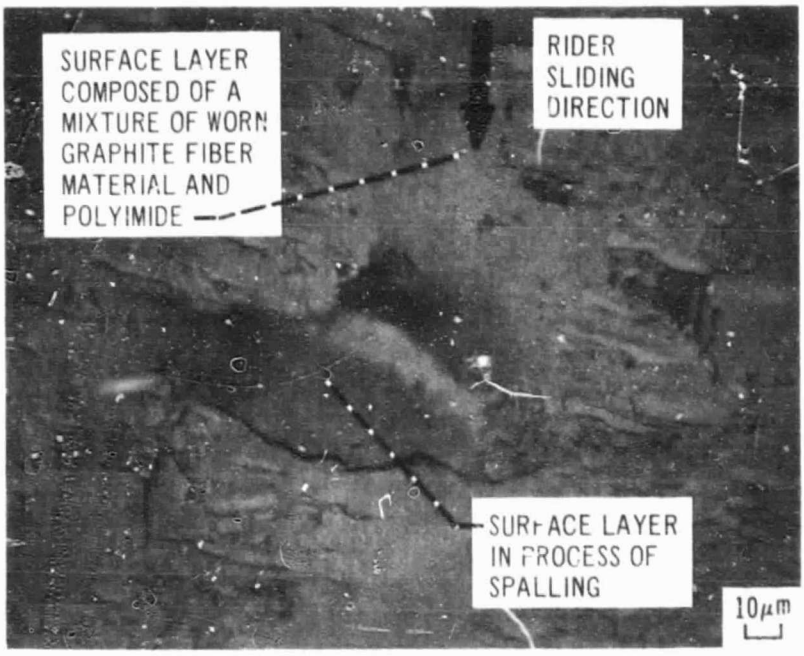

Figure 19. - Photomicrograph of typical wear surface morphology at 25° C on the graphite fiber reinforced polyimide composite.

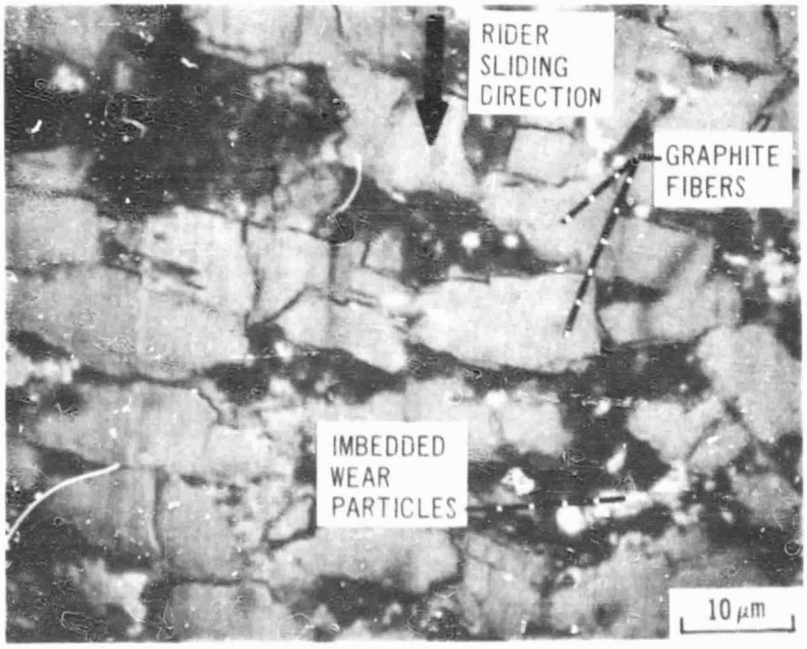

Figure 20. - Photomicrographs of typical wear surface morphology at 550° C in moist air of GFRPI composites.

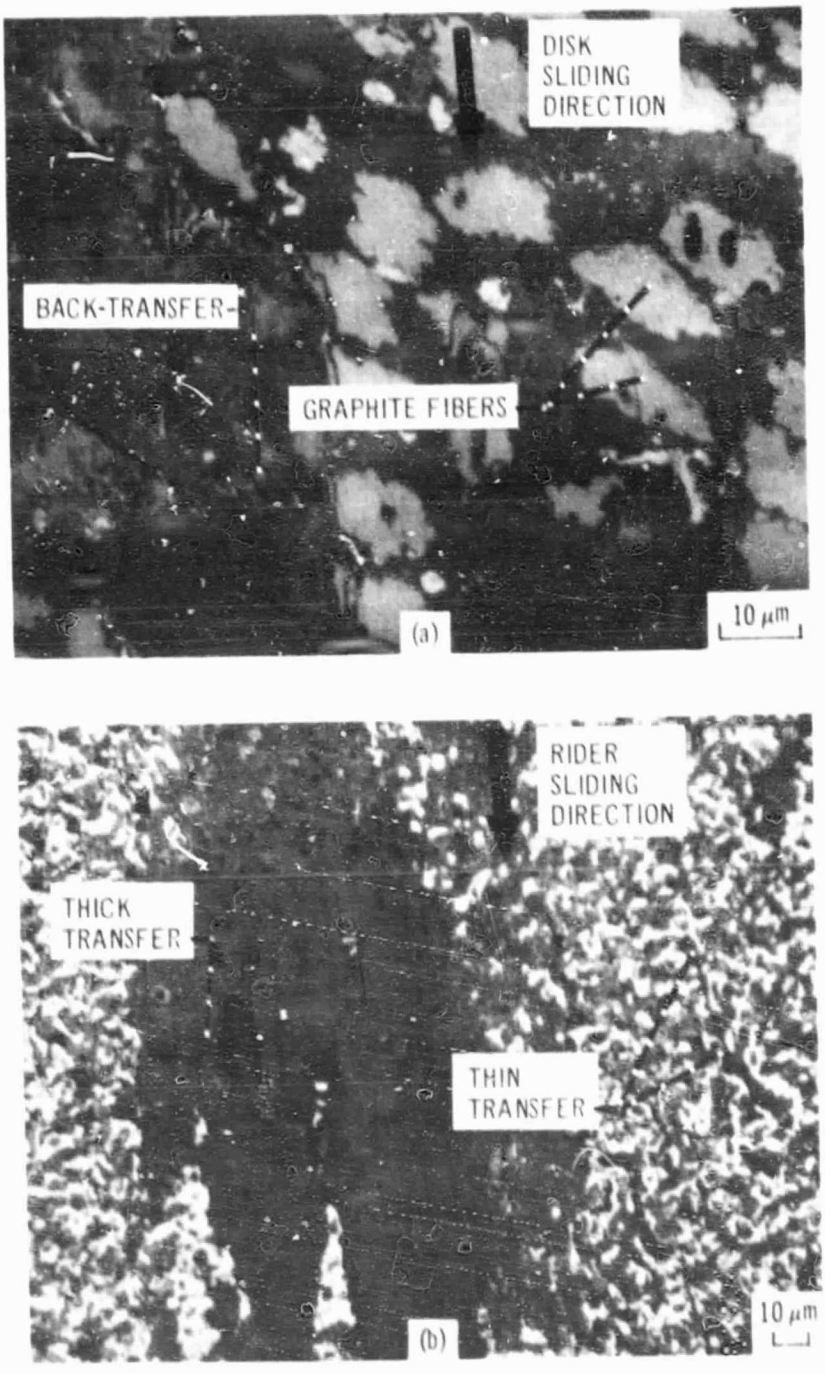

(a) GFRPI composite pin.

(b) Transfer to 440C HT steel counterface.

Figure 21. - Photomicrographs of typical sliding surface morphology for a GFRPI composite pin sliding against a 440C HT stainless steel counterface in moist air at 25° C.